# Multicritical Phase Diagrams of the Blume-Emery-Griffiths Model with Repulsive Biquadratic Coupling

William Hoston and A. Nihat Berker

*Department of Physics, Massachusetts Institute of Technology, Cambridge, Massachusetts 02139*

(Received 13 June 1991)

Six new phase diagrams, including a novel multicritical topology and two new ordered phases, high-entropy ferrimagnetic and antiquadrupolar, are found in the spin-1 Ising model with only nearest-neighbor interactions, for negative biquadratic couplings. Thus, the global phase diagram of this simple spin system includes nine distinct topologies and three ordered phases. It is indicated that these results, obtained by mean-field theory, are applicable to three-dimensional systems.

PACS numbers: 75.10.Hk, 05.70.Fh, 64.60.Kw, 75.50.Gg

The Blume-Emery-Griffiths (BEG) model [1,2] is the most general spin-1 Ising model with nearest-neighbor interactions and up-down symmetry, with Hamiltonian

$$-\beta\mathcal{H}=J\sum_{\langle ij\rangle}s_is_j+K\sum_{\langle ij\rangle}s_i^2s_j^2-\Delta\sum_i s_i^2\,, \tag{1}$$

composed, respectively, of bilinear interaction, biquadratic interaction, and crystal-field terms. In Eq. (1), the spin $s_i=0,\pm 1$ is at each site $i$ of a lattice, each site has $z$ nearest neighbors, and $\langle ij\rangle$ denotes summation over all nearest-neighbor pairs of sites. First studied [1] in the context of superfluidity and phase separation in helium mixtures, this model has been extended to solid-liquid-gas systems [3], multicomponent fluid and liquid crystal mixtures [3], microemulsions [4], and semiconductor alloys [5]. In fact, the BEG model is, much more generally, the basic model for systems in which the phase transitions can be driven by symmetry-breaking fluctuations ($s_i=\pm 1$) and by density fluctuations ($s_i^2=1,0$). The BEG model has moreover played an important guiding role in the development of microscopic models for adsorbed systems [6] and in the renormalization-group theory of Potts transitions [7].

The BEG model, for positive ($J,K>0$) interactions, has been globally analyzed by mean-field [1] and renormalization-group [2] methods. Antiferromagnetic bilinear ($J<0$) interactions are simply mapped onto the ferromagnetic cases ($J\rightarrow -J$) by redefining the spin direction on one sublattice, in lattices that are decomposed into two sublattices, to which we limit ourselves presently. Thus, with no loss of generality, we discuss non-negative $J$ in the remainder of this article. The case of repulsive biquadratic ($K<0$) interactions [8,9], however, is drastically and richly different, as will be seen from the global study reported in this paper. Six new phase diagrams, featuring two new phases and a novel multicritical topology, are thus obtained. One of these phases has high entropy content and spans only intermediate temperatures. Attention has been drawn independently to the negative biquadratic interactions region of the BEG model through a connection to the $t$-$J$ model of electronic conduction [10] and through the applicability to ordering in semiconductor alloys [11].

Our study is a mean-field theory, based on the Gibbs inequality for the free energy [12],

$$F\leq \mathrm{Tr}\rho\mathcal{H}+\beta^{-1}\mathrm{Tr}\rho\ln\rho\,, \tag{2}$$

where $\rho$ is any acceptable density matrix (i.e., Hermitian, non-negative, and normalized). We minimized the right side of this equation for the most general density matrix that is factored into single-site density matrices, allowing for sublattice symmetry breaking. The resulting phases are variously distinguished by *four* order parameters,

$$M_A=\langle s_i\rangle_A,\quad M_B=\langle s_i\rangle_B,\quad Q_A=\langle s_i^2\rangle_A,\quad Q_B=\langle s_i^2\rangle_B\,, \tag{3}$$

where $A$ and $B$ refer to the two sublattices. These subscripts will not be displayed when sublattice symmetry is not broken. Classical mean-field theories are expected to be valid in higher spatial dimensions. From connections we make to Potts antiferromagnetism, it will be seen below that the new multicritical structures should already occur in three dimensions ($d=3$).

The global phase diagram is conveyed in Figs. 1(a)–1(i), which are the distinct constant-$K/J$ cross sections in the temperature ($1/zJ$) versus chemical potential ($\Delta/zJ$) variables. The corresponding cross sections in temperature versus density $\langle s_i^2\rangle$ are given in Figs. 2(a)–2(i). We first briefly review the cross sections for $K/J\geq 0$: For large positive values of $K/J$ [e.g., Fig. 1(a)], a critical line terminates at a critical end point ($E$) on a line of first-order transitions, which itself terminates at a critical point ($C$). The ferromagnetic phase ($f$) is distinguished by $M\neq 0$. The disordered phase ($d$) exhibits distinct dense and dilute versions coexisting on the higher-temperature segment of the first-order line. For values of $K/J$ close to zero [e.g., Fig. 1(c)], the critical line meets the first-order line at a tricritical point ($T$). In between these two topologies, for $K/J$ values close to 3, a phase diagram topology with a tricritical point ($T$), a triple point ($R$), and a critical point ($C$) occurs [e.g., Fig. 1(b)].

Six new phase diagram topologies were found when we extended the $K/J$ values to negative values: (1) The tricritical phase diagram develops a *doubly reentrant* topology [e.g., Fig. 1(d)]. As temperature is lowered at fixed

 

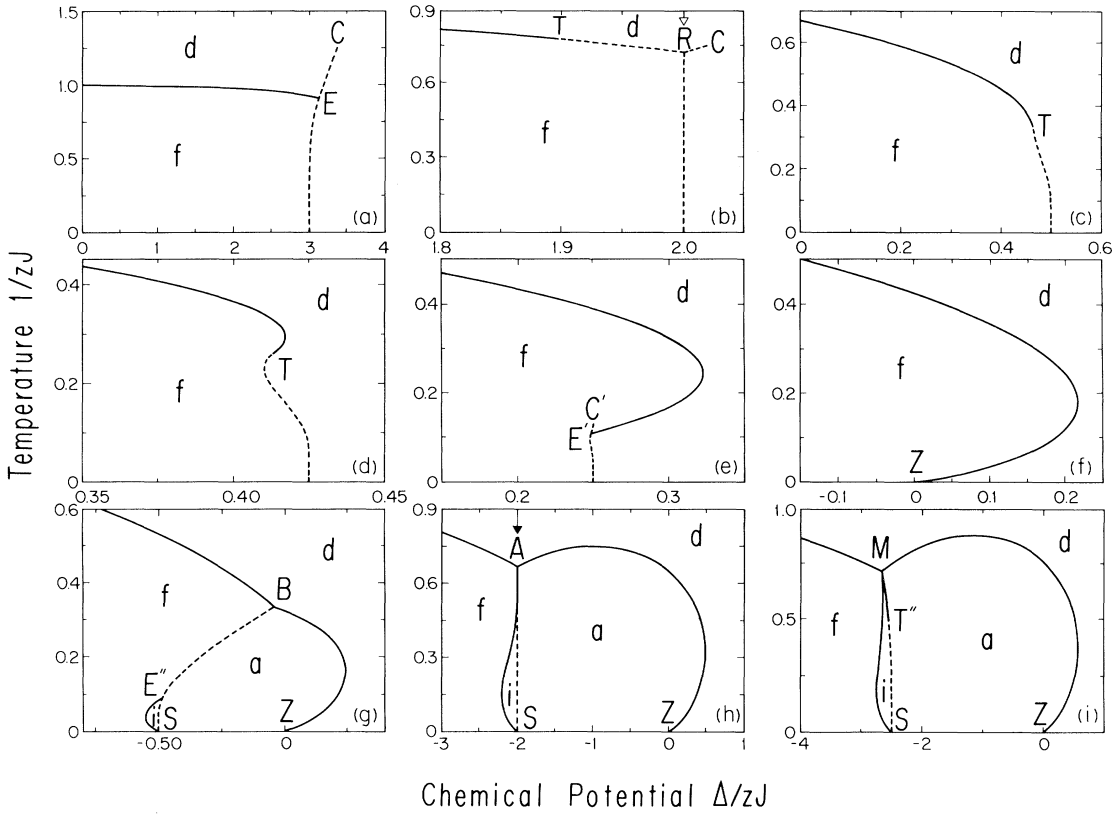


FIG. 1. Phase diagrams for $K/J$ values of (a) 5, (b) 3, (c) 0, (d) $-0.15$, (e) $-0.5$, (f) $-1$, (g) $-1.5$, (h) $-3$, and (i) $-3.5$. Disordered ($d$), ferromagnetic ($f$), ferrimagnetic ($i$), and antiquadrupolar ($a$) phases are found. Dashed and solid lines, respectively, indicate first- and second-order phase transitions. The special points are critical ($C$,$C'$), critical end point ($E$,$E'$,$E''$), zero-temperature critical ($Z$), zero-temperature highly degenerate ($S$), bicritical ($B$), tricritical ($T$,$T''$), tetracritical ($M$), multicritical ($A$), and triple ($R$). The open and solid arrows, respectively, indicate the three-state Potts ferromagnetic and antiferromagnetic subspaces.

chemical potential, the disordered-ferromagnetic-disordered-ferromagnetic sequence of phases is encountered. This topology terminates by a *fourth-order point* (see below) occurring at the stability limit of tricriticality, $K/J=1/\sqrt{10}-1/2\approx -0.18$. (2) For $1/\sqrt{10}-1/2>K/J>-1$, there occur a critical end point ($E'$) and, *inside the ferromagnetic phase*, a first-order line segment terminating at a critical point ($C'$) [e.g., Fig. 1(e)]. Thus, in this case, the ferromagnetic phase exhibits distinct dense and dilute versions coexisting on the higher-temperature segment of the first-order line. (These coexisting phases, four in number when up or down magnetization is taken into account, are the phases that become mutually critical at the fourth-order point mentioned above.) We distinguish this "internal" critical-point–end-point structure from the "external" critical-point–end-point structure of the large positive $K/J$ values. As $K/J$ approaches $-1$, this internal structure collapses toward zero temperature and thus disappears at $K/J=-1$. (3) At $K/J=-1$, a singly reentrant critical line reaches zero temperature [Fig. 1(f)] at the point $Z$, which, as a critical point characterized by fluctuations at zero temperature, should be in a different universality class than the critical line it terminates.

For $K/J<-1$, two new ordered phases emerge. The *ferrimagnetic* phase [8] is characterized by nonzero magnetization and sublattice symmetry breaking:

$$0\neq M_A\neq M_B\neq 0,\quad Q_A\neq Q_B\,. \tag{4}$$

This ferrimagnetic phase has high entropy content and spans in field-space intermediate temperatures only. The *antiquadrupolar* phase [8] has sublattice symmetry breaking, but zero magnetization:

$$M_A=M_B=0,\quad Q_A\neq Q_B\,. \tag{5}$$

(4) Thus, for $-1>K/J>-3$, the ferromagnetic ($f$) and antiquadrupolar ($a$) phases are separated from the disordered phase by two critical lines that meet at a bicritical point [9] ($B$) [e.g., Fig. 1(g)]. The antiquadrupolar phase is separated from the nonzero-magnetization phases by the first-order line that terminates at the bicritical point. The ferromagnetic ($f$) and ferrimagnetic ($i$)

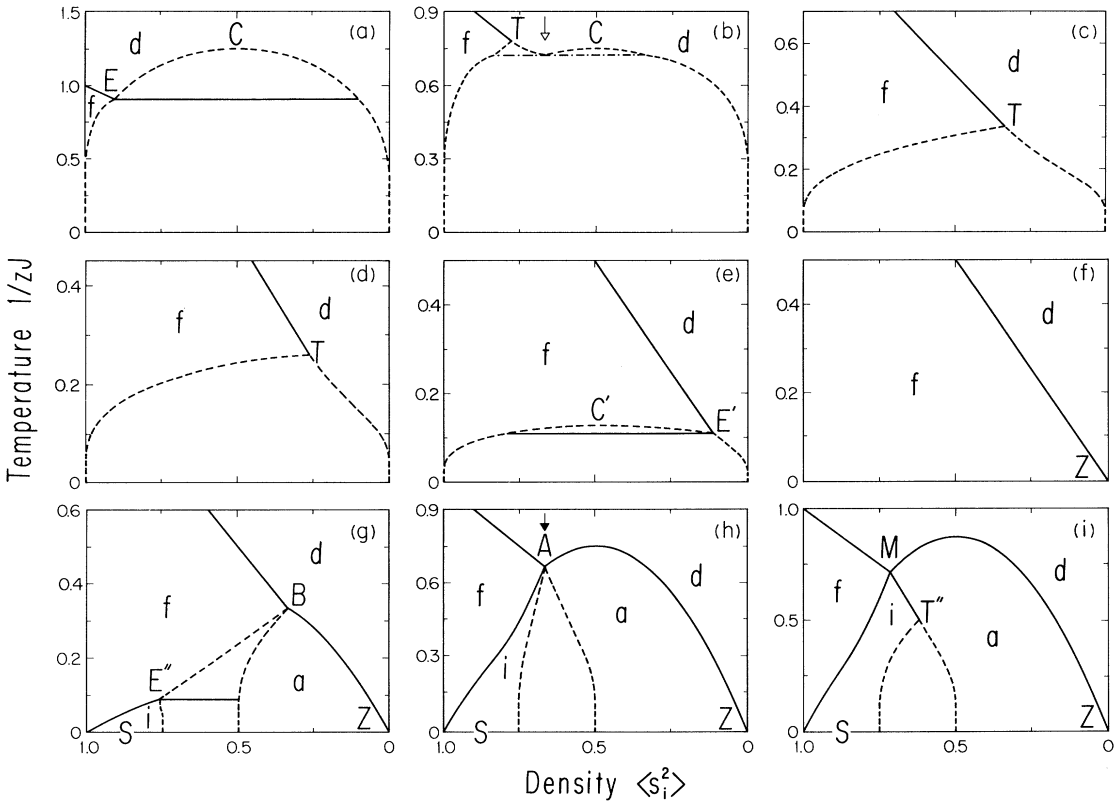


FIG. 2. Phase diagrams in temperature and density corresponding to Fig. (1). Unmarked regions are the coexistence regions of the phases on each side. Dashed and solid lines, respectively, indicate coexistence boundaries and second-order boundaries. The open and solid arrows, respectively, indicate the three-state Potts ferromagnetic and antiferromagnetic subspaces.

phases are separated by another critical line terminating at the critical end point $E''$ on the first-order line. The zero temperature ($1/zJ=0$), $\Delta/zJ=K/J+1$, and $K/J \leq -1$ points ($S$), where the three ordered phases meet, are points of high degeneracy, namely, the saturated ferromagnetic ($M_A=Q_A=M_B=Q_B=1$) and antiquadrupolar ($Q_A=1, M_A=M_B=Q_B=0$) states, and the continuum of ferrimagnetic macroscopic states ($M_A=Q_A=1$, $1/2<M_B=Q_B<1$) minimize the mean-field free energy, as seen by the associations of Figs. 1 and 2. As $K/J$ approaches $-3$, the critical end point approaches the bicritical point.

(5) At $K/J=-3$ [Fig. 1(h)], these two points merge. A novel multicritical topology is found around this point $A$, where three critical lines and one first-order line meet. The first-order line occurs at constant chemical potential (and the low-temperature critical line reaches $A$ with vertical slope). In fact, on the locus $K/J=-3$, $\Delta/zJ=-2$, which contains the first-order line, the BEG model reduces to the antiferromagnetic three-state Potts model [13]:

$$-\beta\mathcal{H}=-3J\sum_{\langle ij\rangle}\delta_{s_i s_j}, \quad J>0, \tag{6}$$

where $\delta_{s_i s_j}=1$ (0) for $s_i=s_j$ ($s_i \neq s_j$). Attention was first drawn to antiferromagnetic $q$-state Potts models when renormalization-group analysis [14] indicated that, for spatial dimensionality $d$ above a lower-critical value of $d_c$, a finite-temperature phase transition occurs, with $d_c \approx 2.8$ for $q=3$. Subsequent Monte Carlo simulation [15] confirmed the finite-temperature phase transition and established the local ordering degrees of freedom, namely, local sublattice densities such that one sublattice is deficient in one of the three spin states and the other sublattice is rich in this spin state. Since this symmetry breaking can be achieved in six equivalent ways, the ordering involves the coexistence of six degenerate phases. In fact, these six degenerate phases do coexist on the low-temperature segment of the antiferromagnetic Potts subspace in Fig. 1(h), as the two coexisting degenerate phases of the antiquadrupolar phase and the four coexisting degenerate phases of the ferrimagnetic phase coexist at the first-order line on this segment [also see the densities in Fig. 2(h)]. Conversely, the finite-temperature phase transition [14,15] of the antiferromagnetic Potts model in $d=3$ dictates the occurrence of the ferrimagnetic phase in the Blume-Emery-Griffiths model. Momentum-space renormalization-group $\epsilon=4-d$ expansion assigned [16] the $n=2$ universality class to the transition of

the antiferromagnetic three-state Potts model. However, more recent Monte Carlo simulation [17] in $d=3$ indicates a new universality class.

(6) For $K/J < -3$, a tetracritical point $M$ occurs, where four critical lines meet with different slopes [e.g., Fig. 1(i)]. The ferrimagnetic-antiquadrupolar critical line terminates, at a lower temperature, at another tricritical point ($T''$), beyond which the transition is first order. Thus, this *tricriticality is totally inside ordered phases.* Finally, as $K/J$ is made more negative, the tricritical point $T''$ moves to lower temperatures and the antiquadrupolar phase bulges to higher temperatures.

It is thus seen that a large variety of phase transition phenomena are introduced to the simplest model incorporating both orientational and density degrees of freedom, when the latter are coupled by a repulsive interaction.

Support by the Fermi National Accelerator Laboratory and by a Patricia Harris Fellowship is gratefully acknowledged by W.H. This research was supported by NSF Grant No. DMR-90-22933 and by JSEP Contract No. DAAL 03-89-C0001.

[1] M. Blume, V. J. Emery, and R. B. Griffiths, Phys. Rev. A **4**, 1071 (1971).

[2] A. N. Berker and M. Wortis, Phys. Rev. B **14**, 4946 (1976).

[3] J. Lajzerowicz and J. Sivardière, Phys. Rev. A **11**, 2079 (1975); J. Sivardière and J. Lajzerowicz, *ibid.* **11**, 2090 (1975); **11**, 2101 (1975).

[4] M. Schick and W.-H. Shih, Phys. Rev. B **34**, 1797 (1986).

[5] K. E. Newman and J. D. Dow, Phys. Rev. B **27**, 7495 (1983).

[6] A. N. Berker, S. Ostlund, and F. A. Putnam, Phys. Rev. B **17**, 3650 (1978).

[7] B. Nienhuis, A. N. Berker, E. K. Riedel, and M. Schick, Phys. Rev. Lett. **43**, 737 (1979).

[8] H. H. Chen and P. M. Levy, Phys. Rev. B **7**, 4267 (1973).

[9] M. Tanaka and T. Kawabe, J. Phys. Soc. Jpn. **54**, 2194 (1985).

[10] S. A. Kivelson, V. J. Emery, and H. Q. Lin, Phys. Rev. B **42**, 6523 (1990).

[11] K. E. Newman and X. Xiang, Bull. Am. Phys. Soc. **36**, 599 (1991).

[12] H. Falk, Am. J. Phys. **38**, 858 (1970).

[13] The *ferromagnetic* three-state Potts model, on the other hand, obtains for $K/J=3$, $\Delta/zJ=2$ (see Ref. [2]). This subspace is contained in Fig. 1(b).

[14] A. N. Berker and L. P. Kadanoff, J. Phys. A **13**, L259 (1980).

[15] J. R. Banavar, G. S. Grest, and D. Jasnow, Phys. Rev. Lett. **45**, 1424 (1980).

[16] J. R. Banavar, G. S. Grest, and D. Jasnow, Phys. Rev. B **25**, 4639 (1982).

[17] Y. Ueno, G. Sun, and I. Ono, J. Phys. Soc. Jpn. **58**, 1162 (1989).